

Flux growth and structure of two compounds with the EuIn_2P_2 structure type, AIn_2P_2 ($A = \text{Ca}$ and Sr), and a new structure type, BaIn_2P_2

Japheth F. Rauscher,^a Cathie L. Condrón,^a Tanya Beault,^a Susan M. Kauzlarich,^{a*} Newell Jensen,^b Peter Klavins,^b Samuel MaQuilon,^b Zachary Fisk^b and Marilyn M. Olmstead^a

^aDepartment of Chemistry, University of California, One Shields Avenue, Davis, CA 95616, USA, and ^bDepartment of Physics, University of California, One Shields Avenue, Davis, CA 95616, USA

Correspondence e-mail: smkauzlarich@ucdavis.edu

Received 12 July 2009

Accepted 5 September 2009

Online 30 September 2009

Single crystals of the new Zintl phases AIn_2P_2 [$A = \text{Ca}$ (calcium indium phosphide), Sr (strontium indium phosphide) and Ba (barium indium phosphide)] have been synthesized from a reactive indium flux. CaIn_2P_2 and SrIn_2P_2 are isostructural with EuIn_2P_2 and crystallize in the space group $P6_3/mmc$. The alkaline earth cations A are located at a site with $\bar{3}m$ symmetry; In and P are located at sites with $3m$ symmetry. The structure type consists of layers of A^{2+} cations separated by $[\text{In}_2\text{P}_2]^{2-}$ anions that contain $[\text{In}_2\text{P}_6]$ eclipsed ethane-like units that are further connected by shared P atoms. This yields a double layer of six-membered rings in which the In–In bonds are parallel to the c axis and to one another. BaIn_2P_2 crystallizes in a new structure type in the space group $P2_1/m$ with $Z = 4$, with all atoms residing on sites of mirror symmetry. The structure contains layers of Ba^{2+} cations separated by $[\text{In}_2\text{P}_2]^{2-}$ layers of staggered $[\text{In}_2\text{P}_6]$ units that form a mixture of four-, five- and six-membered rings. As a consequence of this more complicated layered structure, both the steric and electronic requirements of the large Ba^{2+} cation are met.

Comment

Layered ternary compounds, AB_2X_2 ($A = \text{rare earth or alkaline earth metal}$; $B = \text{main group, metalloid}$; $X = \text{main group 14–17 element}$) or 1–2–2 phases, favor the ThCr_2Si_2 ($I4/mmm$) structure type, with the CaAl_2Si_2 structure type ($P\bar{3}m1$) as a distant second (Grytsiv *et al.*, 2002; Hellmann *et al.*, 2007). There are a few other less commonly observed structure types for layered main group metalloids, such as $\alpha\text{-BaCu}_2\text{S}_2$ ($Pnma$; Leoni *et al.*, 2003) observed for BaAl_2Si_2 (Condrón *et al.*, 2007), and EuIn_2P_2 (Jiang & Kauzlarich, 2006). In addition to

layered structure types, there is at least one example of a 1–2–2 phase with a three-dimensional structure, as found in BaGa_2Sb_2 (Kim & Kanatzidis, 2001). More complex two- and three-dimensional structures composed of alkaline earth, In and P have also been reported, such as $\text{Ba}_2\text{In}_5\text{P}_5$ (Mathieu *et al.*, 2008), $\text{Ba}_{14}\text{InP}_{11}$ (Carrillo-Cabrera *et al.*, 1996) and $\text{Ba}_3\text{In}_2\text{P}_4$ (Sommer *et al.*, 1998).

The rare earth Zintl phase EuIn_2P_2 contains two-dimensional layers of Eu^{2+} cations dispersed between layers of $[\text{In}_2\text{P}_2]^{2-}$ anions. EuIn_2P_2 has been shown to exhibit colossal magnetoresistance (Jiang & Kauzlarich, 2006). The temperature-dependent magnetoresistance and the magneto-optical behavior of this compound suggest interaction between conduction electrons and local spins (Jiang & Kauzlarich, 2006; Pfuner *et al.*, 2008). The alkaline earth analogs of EuIn_2P_2 were prepared in order to provide a nonmagnetic analog for heat capacity and electrical transport studies. The existence of the Sr analog has been alluded to in a recent publication (Mathieu *et al.*, 2008), although the structural details were not provided. Here, two new members of the $P6_3/mmc$ structure type are presented, along with one new structure type, $P2_1/m$. Both structures can be described as composed of In_2P_6 ethane-like moieties (either eclipsed or staggered) connected through the P atoms in such a fashion as to form layers separated by alkaline earth cations.

CaIn_2P_2 and SrIn_2P_2 are isostructural in the space group $P6_3/mmc$. A view of SrIn_2P_2 emphasizing the layered structure is provided in Fig. 1. AIn_2P_2 ($A = \text{Ca}$ and Sr) contains alter-

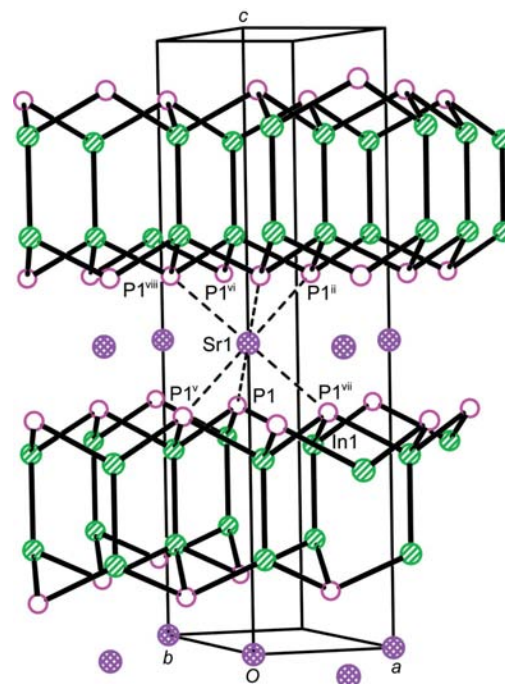


Figure 1
The crystal structure of SrIn_2P_2 , viewed down the $[110]$ direction, showing the $[\text{In}_2\text{P}_2]^{2-}$ layers and the trigonal antiprismatic coordination of Sr. Atoms are shown at an arbitrary size. [Symmetry codes: (v) $x - 1, y - 1, z$; (ii) $-x + 1, -y + 1, -z + 1$; (vi) $-x, -y, -z + 1$; (vii) $x, y - 1, z$; (viii) $-x, -y + 1, -z + 1$.]

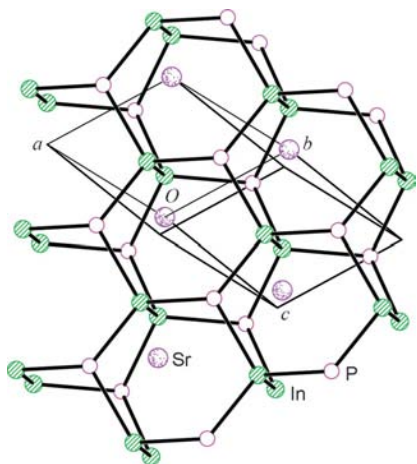


Figure 2
A view approximately perpendicular to the InP layer of SrIn_2P_2 , showing the presence of six-membered rings and eclipsed P_3InInP_3 units. The Sr^{2+} cations are symmetrically placed above the six-membered rings but are shown offset for clarity.

nating layers of $[\text{In}_2\text{P}_2]^{2-}$ that are parallel to (001) and charge balanced by A^{2+} cationic layers stacked along the c axis. The alkaline earth element resides on Wyckoff position a (multiplicity 2) with $\bar{3}m$ site symmetry. As shown in Fig. 1, its coordination environment consists of six P atoms in a trigonal antiprismatic arrangement. The In cation resides on Wyckoff position f (multiplicity 4) with $3m$ symmetry. There are three surrounding P atoms in a pyramidal arrangement and an apical In cation. The centroid of the In–In bond is a site of $\bar{6}m2$ (D_{3h}) symmetry; thus, the ethane-related $\text{P}_3\text{In}–\text{InP}_3$ unit has eclipsed P atoms. Each P atom [also at Wyckoff position f (multiplicity 4) with $3m$ symmetry] has three equal bonds to In, as well as three equal bonds to Ca (Sr). The $\text{P}_3\text{In}–\text{InP}_3$ units are connected in parallel *via* bridging P atoms to form a double layer of six-membered rings. The Ca or Sr cations are centered above each ring and form layers above and below each double layer of rings, as shown in Fig. 2.

The In–P bonds are considered to be covalent, whereas the In–Ca (Sr) interactions are electrostatic in origin. By Zintl electron counting (Kauzlarich, 1996), each P atom has a lone pair. The lone pair may have largely an s character, since its simultaneous interaction with three Sr atoms (Ca atoms) shows it to be nondirectional. The majority of the bond distances increase from the Ca to the Sr compound, as expected; the In–Inⁱ [symmetry code: (i) $x, y, -z + \frac{1}{2}$] distances are equal within experimental error for both compounds. The previously reported Eu phase contains intermediate distances (Jiang & Kauzlarich, 2006).

BaIn_2P_2 adopts a new structure type with greater complexity and geometric distortion in the space group $P2_1/m$. Each atom resides on a crystallographic mirror plane. The structure is similar to CaIn_2P_2 and SrIn_2P_2 in that it contains alternating layers of $[\text{In}_2\text{P}_2]^{2-}$ sheets, parallel to the (101) plane, that are charge balanced by A^{2+} cationic layers, as shown in Fig. 3. The In–In distances of 2.7625 (19) and 2.7620 (13) Å, corresponding to CaIn_2P_2 and SrIn_2P_2 ,

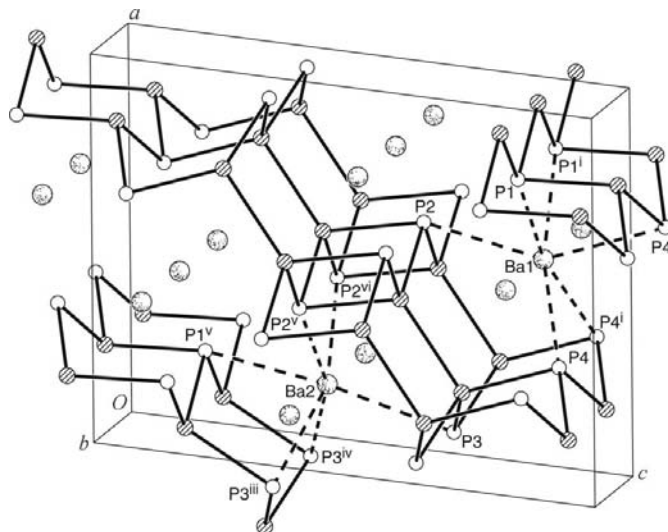


Figure 3
The crystal structure of BaIn_2P_2 , viewed down the b axis. For clarity, Ba atoms are shown as dotted circles, P atoms as open circles and In atoms as shaded bottom left to upper right circles. Dashed lines show the six-coordinate environment for Ba1 and Ba2. [Symmetry codes: (i) $x, y - 1, z$; (ii) $-x + 1, -y + 1, -z + 2$; (iii) $-x, -y + 1, -z + 1$; (iv) $-x, -y + 1, -z + 1$; (v) $-x + 1, -y + 1, -z + 1$; (vi) $-x + 1, -y, -z + 1$.]

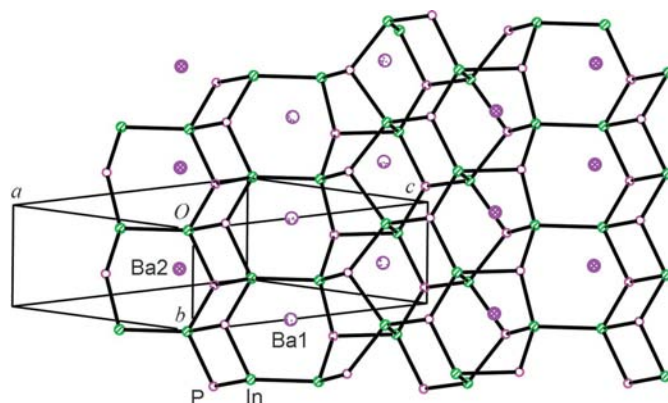


Figure 4
A view approximately perpendicular to the InP layer of BaIn_2P_2 . The positioning of Ba^{2+} cations above the four-, five- and six-membered rings is shown. In order to distinguish between Ba1 and Ba2, Ba1 cations are shown with dotted circles and Ba2 cations are shown with cross-hatched circles.

respectively, are bracketed by the two In–In bond distances of 2.7460 (10) [$\text{In}2–\text{In}3^{\text{vi}}$; symmetry code: (vi) $2 - x, -y, 2 - z$] and 2.8161 (10) Å ($\text{In}1–\text{In}4$) observed in BaIn_2P_2 . There are two crystallographic sites for Ba cations in this structure. Each Ba is coordinated by six P atoms in a distorted trigonal antiprismatic arrangement, as shown in Fig. 3. The In coordination in BaIn_2P_2 is similar to that in CaIn_2P_2 and SrIn_2P_2 in that it is comprised of another In cation and three P atoms, forming a $\text{P}_3\text{In}–\text{InP}_3$ unit. However, in this structure, the ethane-like moiety is staggered and has noncrystallographic D_{3d} symmetry. The $[\text{In}_2\text{P}_2]^{2-}$ layers are markedly different in BaIn_2P_2 and consist of four-, five- and six-membered rings. A

view roughly perpendicular to the InP layer (Fig. 4) emphasizes this difference when compared with Fig. 2. The lower symmetry in the layer in BaIn_2P_2 is likely related to the necessity to accommodate the larger Ba^{2+} cation (Shannon, 1976). If one assumes that the separation between cations is linked to the repeat distances of the six-membered $(\text{InP})_3$ rings [4.0220 (17) Å in CaIn_2P_2 and 4.0945 (16) Å in SrIn_2P_2], it is apparent that the EuIn_2P_2 structure type cannot accommodate Ba. In BaIn_2P_2 , the shortest $\text{Ba}\cdots\text{Ba}$ distance is 4.1789 (3) Å.

There are many examples where the identity of the cation provides different structures for isoelectronic series of compounds and this is also the case for Zintl and intermetallic phases (Kauzlarich, 1996; Nesper, 1990). For example, AMn_2P_2 ($A = \text{Sr}$ and Ba) assumes different structure types depending on the identity of the cation: SrMn_2P_2 crystallizes in the CaAl_2Si_2 structure type, whereas BaMn_2P_2 crystallizes in the ThCr_2Si_2 structure type (Brock *et al.*, 1994). This was attributed to the difference in cation coordination: octahedral for the cation site in CaAl_2Si_2 versus cubic in the ThCr_2Si_2 structure type. Electronic considerations have been shown to play an important role in dictating structure and properties for other isoelectronic series (Alemany *et al.*, 2008; Xia & Bobev, 2007, 2008; Kim *et al.*, 2008). For AIn_2P_2 ($A = \text{Ca}$ and Sr), the EuIn_2P_2 structure type, the six-membered ring structure of the nonmetal layer cannot accommodate the size of the Ba cation and a new structure type is adopted.

Of the published structures of the combination of alkaline earth cation and group 13 and 15 elements, $\text{Ba}_2\text{In}_5\text{P}_5$ is a recent example of a layered structure that is built up from ethane-like moieties (Mathieu *et al.*, 2008). The bond distances and angles in this compound are very similar to those observed in BaIn_2P_2 presented herein. The structure of $\text{Ba}_2\text{In}_5\text{P}_5$ can be described as containing two staggered ethane-like moieties similar to that observed in the BaIn_2P_2 structure type, with the In—In bonds arranged parallel to each other and connected *via* P atoms. However, in $\text{Ba}_2\text{In}_5\text{P}_5$, two of the parallel moieties are joined through a P atom by a highly distorted InP_4 tetrahedron.

The ethane-like moiety is also observed in the three-dimensional framework structures of BaGa_2Sb_2 (Kim & Kanatzidis, 2001) and $\text{Ba}_3\text{Ga}_4\text{Sb}_5$ (Park *et al.*, 2003). Both BaGa_2Sb_2 and $\text{Ba}_3\text{Ga}_4\text{Sb}_5$ adopt unique structure types that contain tunnels wherein the Ba^{2+} cations reside (Kim & Kanatzidis, 2001; Park *et al.*, 2003).

AIn_2P_2 ($A = \text{Ca}$, Sr and Ba) can be considered Zintl phases where there is electrostatic bonding between the alkaline earth cation and the layered anion (Kauzlarich, 1996). The basic building block of the ethane-like moiety is a common element in compounds composed of alkaline earth, group 13 and group 15 elements. Similar to the molecule ethane, this moiety can have a staggered or eclipsed conformation, however, it has a strong preference for a staggered conformation. This moiety is connected through shared P atoms to form extended structures in these compounds. The interaction of the P atoms with the cation, rather than the In—In bond length, may determine whether the moiety is eclipsed or

staggered, as the In—In bond is both the shortest and longest in the BaIn_2P_2 compound (moiety is staggered) compared with the Ca (Sr) compounds (moiety is eclipsed).

Experimental

AIn_2P_2 crystals were grown by reaction of the pure elements in an alumina crucible with an $A:\text{In}:\text{P}$ molar ratio of 3:110:6, where $A = \text{Ca}$, Sr or Ba . The metals, *viz.* Ca (Aldrich, 99.99% purity), Sr (Aldrich, 99% purity), Ba (Aldrich, 99% purity) and In (Cerac, 99.99% purity), were cut into small pieces and layered in a 5 ml crucible with indium on the top and bottom, and sealed under vacuum in quartz tubes. All materials were handled under an inert atmosphere or under vacuum. The reaction contents were heated in a programmable furnace at a rate of 60 K h^{-1} to 1373 K, maintained at that temperature for 16 h, cooled at a rate of 2 K h^{-1} to 1146 K, maintained at that temperature for 24 h and centrifuged to remove molten In flux. The crystals were then removed after breaking the quartz jacket in air. In the cases of Ca and Sr, the reactions yielded a few highly reflective black plate-like crystals on the sides and bottom of the crucible. In the Ba reactions, larger yields of black needle-shaped crystals were found within the crucible. All the crystals were found to be air stable. Attempts were made to increase the yield by decreasing the flux ratio, but this had the opposite effect of lowering the yield. In the case of Ba, some crystals of $\text{Ba}_2\text{In}_5\text{P}_5$ (Mathieu *et al.*, 2008) were also present. The $\text{Ba}_2\text{In}_5\text{P}_5$ phase is reported to be air sensitive and decomposed upon exposure to air, whereas the BaIn_2P_2 crystals remained stable in air. The best formed crystals and highest yields of the 1–2–2 phases were for Ba.

The chemical composition of the Ba crystals was verified with an SEM (scanning electron microscopy) microprobe on a single crystal using a Camera SX-100 Electron Probe Microanalyzer equipped with a wavelength-dispersive spectrometer and calibrated standards. The samples were prepared by embedding the crystals in epoxy and polishing to ensure smooth surfaces. Each sample was scanned with a spot size of 1 μm and data were collected at five to eight points along its surface. Composition totals for all points summed to 100%. The compositions were calculated as the average of the five points and provided the composition $\text{Ba}_{1.00(4)}\text{In}_{2.023(6)}\text{P}_{2.020(3)}$, in good agreement with the refined structure.

CaIn_2P_2

Crystal data

CaIn_2P_2	$Z = 2$
$M_r = 331.66$	Mo $K\alpha$ radiation
Hexagonal, $P6_3/mmc$	$\mu = 10.97 \text{ mm}^{-1}$
$a = 4.0220$ (17) Å	$T = 90 \text{ K}$
$c = 17.408$ (8) Å	$0.42 \times 0.40 \times 0.12 \text{ mm}$
$V = 243.87$ (18) Å ³	

Data collection

Bruker SMART 1000 diffractometer	3448 measured reflections
Absorption correction: multi-scan (SADABS; Sheldrick, 2003)	179 independent reflections
$T_{\min} = 0.021$, $T_{\max} = 0.268$	153 reflections with $I > 2\sigma(I)$
	$R_{\text{int}} = 0.055$

Refinement

$R[F^2 > 2\sigma(F^2)] = 0.028$	10 parameters
$wR(F^2) = 0.073$	$\Delta\rho_{\max} = 1.14 \text{ e \AA}^{-3}$
$S = 1.27$	$\Delta\rho_{\min} = -2.15 \text{ e \AA}^{-3}$
179 reflections	

Table 1

 Selected geometric parameters (Å, °) for CaIn_2P_2 .

Ca1—P1	2.936 (2)	In1—In1 ⁱ	2.7625 (19)
In1—P1	2.6021 (16)		
P1—Ca1—P1 ⁱⁱ	93.54 (7)	P1—In1—In1 ⁱ	116.82 (6)
P1 ⁱⁱⁱ —In1—P1	101.22 (7)	In1 ^{iv} —P1—In1	101.22 (7)

 Symmetry codes: (i) $x, y, -z + \frac{1}{2}$; (ii) $-x + 1, -y + 1, -z + 1$; (iii) $x + 1, y, z$; (iv) $x, y + 1, z$.

SrIn_2P_2

Crystal data

SrIn_2P_2	$Z = 2$
$M_r = 379.20$	Mo $K\alpha$ radiation
Hexagonal, $P6_3/mmc$	$\mu = 19.55 \text{ mm}^{-1}$
$a = 4.0945 (16) \text{ \AA}$	$T = 90 \text{ K}$
$c = 17.812 (7) \text{ \AA}$	$0.34 \times 0.24 \times 0.19 \text{ mm}$
$V = 258.61 (18) \text{ \AA}^3$	

Data collection

Bruker SMART 1000 diffractometer	3694 measured reflections
Absorption correction: multi-scan (SADABS; Sheldrick, 2003)	189 independent reflections
$T_{\min} = 0.014, T_{\max} = 0.057$	168 reflections with $I > 2\sigma(I)$
	$R_{\text{int}} = 0.035$

Refinement

$R[F^2 > 2\sigma(F^2)] = 0.015$	10 parameters
$wR(F^2) = 0.037$	$\Delta\rho_{\text{max}} = 0.60 \text{ e \AA}^{-3}$
$S = 1.25$	$\Delta\rho_{\text{min}} = -0.78 \text{ e \AA}^{-3}$
189 reflections	

BaIn_2P_2

Crystal data

BaIn_2P_2	$V = 538.34 (7) \text{ \AA}^3$
$M_r = 428.92$	$Z = 4$
Monoclinic, $P2_1/m$	Mo $K\alpha$ radiation
$a = 9.9652 (8) \text{ \AA}$	$\mu = 16.15 \text{ mm}^{-1}$
$b = 4.1789 (3) \text{ \AA}$	$T = 90 \text{ K}$
$c = 12.9834 (10) \text{ \AA}$	$0.23 \times 0.15 \times 0.09 \text{ mm}$
$\beta = 95.326 (2)^\circ$	

Data collection

Bruker SMART 1000 diffractometer	7899 measured reflections
Absorption correction: multi-scan (SADABS; Sheldrick, 2003)	1753 independent reflections
$T_{\min} = 0.119, T_{\max} = 0.324$	1452 reflections with $I > 2\sigma(I)$
	$R_{\text{int}} = 0.037$

Refinement

$R[F^2 > 2\sigma(F^2)] = 0.038$	62 parameters
$wR(F^2) = 0.093$	$\Delta\rho_{\text{max}} = 2.56 \text{ e \AA}^{-3}$
$S = 1.03$	$\Delta\rho_{\text{min}} = -2.48 \text{ e \AA}^{-3}$
1753 reflections	

There are a number of residual peaks in the final difference map of BaIn_2P_2 that do not appear to be due to twinning or disorder, but may arise from inadequate absorption correction or from stacking faults.

For all compounds, data collection: *SMART* (Bruker, 2003); cell refinement: *SAINTE* (Bruker, 2003); data reduction: *SAINTE*; program(s) used to solve structure: *SHELXS97* (Sheldrick, 2008); program(s) used to refine structure: *SHELXL97* (Sheldrick, 2008);

Table 2

 Selected geometric parameters (Å, °) for SrIn_2P_2 .

Sr1—P1	3.0572 (12)	In1—In1 ⁱ	2.7620 (13)
In1—P1	2.6216 (11)		
P1—Sr1—P1 ⁱⁱ	95.92 (4)	P1—In1—In1 ⁱ	115.62 (3)
P1 ⁱⁱⁱ —In1—P1	102.69 (4)	In1 ^{iv} —P1—In1	102.69 (4)

 Symmetry codes: (i) $x, y, -z + \frac{1}{2}$; (ii) $-x + 1, -y + 1, -z + 1$; (iii) $x + 1, y, z$; (iv) $x, y + 1, z$.

Table 3

 Selected bond lengths (Å) for BaIn_2P_2 .

Ba1—P1	3.218 (2)	In1—P2	2.6283 (17)
Ba1—P2	3.206 (3)	In1—In4	2.8161 (10)
Ba1—P4	3.267 (2)	In2—P1	2.6122 (17)
Ba1—P4 ⁱ	3.290 (3)	In2—P3 ^v	2.673 (3)
Ba2—P1 ^{iv}	3.233 (3)	In2—In3 ^{vi}	2.7460 (10)
Ba2—P2 ⁱⁱ	3.139 (2)	In3—P1	2.587 (3)
Ba2—P3 ⁱⁱⁱ	3.227 (2)	In3—P4 ^{vii}	2.6350 (17)
Ba2—P3	3.438 (3)	In4—P3	2.6296 (18)
In1—P2 ⁱⁱ	2.624 (3)	In4—P4	2.612 (3)

 Symmetry codes: (i) $-x + 1, -y, -z + 2$; (ii) $-x + 1, -y, -z + 1$; (iii) $-x, -y - 2, -z + 1$; (iv) $-x + 1, -y - 1, -z + 1$; (v) $x + 1, y + 1, z$; (vi) $-x + 2, -y, -z + 2$; (vii) $-x + 1, -y - 1, -z + 2$.

molecular graphics: *SHELXTL* (Sheldrick, 2008); software used to prepare material for publication: *SHELXL97*.

This work was supported by the National Science Foundation (grant Nos. DMR-0600742 and DMR-0433560). CLC acknowledges a Tyco Electronics Foundation Fellowship in functional materials. The Bruker SMART 1000 diffractometer was funded in part by NSF Instrumentation grant No. CHE-9808259.

Supplementary data for this paper are available from the IUCr electronic archives (Reference: FA3198). Services for accessing these data are described at the back of the journal.

References

- Aleman, P., Llunell, M. & Canadell, E. (2008). *J. Comput. Chem.* **29**, 2144–2153.
- Brock, S. L., Greedan, J. E. & Kauzlarich, S. M. (1994). *J. Solid State Chem.* **109**, 416–418.
- Bruker (2003). *SMART* and *SAINTE*. Bruker AXS Inc., Madison, Wisconsin, USA.
- Carrillo-Cabrera, W., Somer, M., Peters, K. & von Schnering, H. G. (1996). *Chem. Ber.* **129**, 1015–1023.
- Condron, C. L., Hope, H., Piccoli, P. M. B., Schultz, A. J. & Kauzlarich, S. M. (2007). *Inorg. Chem.* **46**, 4523–4529.
- Grytsiv, A., Kaczorowski, D., Leithe-Jasper, A., Rogl, P., Godart, C., Potel, M. & Noël, H. (2002). *J. Solid State Chem.* **163**, 37–43.
- Hellmann, A., Lohken, A., Wurth, A. & Mewis, A. (2007). *Z. Naturforsch. Teil B*, **62**, 155–161.
- Jiang, J. & Kauzlarich, S. M. (2006). *Chem. Mater.* **18**, 435–441.
- Kauzlarich, S. M. (1996). *Chemistry, Structure, and Bonding of Zintl Phases and Ions*, edited by S. M. Kauzlarich, pp. 245–274. New York: VCH Publishers.
- Kim, S.-J. & Kanatzidis, M. G. (2001). *Inorg. Chem.* **40**, 3781–3785.
- Kim, S. J., Ponou, S. & Fassler, T. F. (2008). *Inorg. Chem.* **47**, 3594–3602.
- Leoni, S., Carrillo-Cabrera, W., Schnelle, W. & Grin, Y. (2003). *Springer Ser. Solid State Sci.* **5**, 139–148.
- Mathieu, J., Achey, R., Park, J.-H., Purcell, K. M., Tozer, S. W. & Latturmer, S. E. (2008). *Chem. Mater.* **20**, 5675–5681.

- Nesper, R. (1990). *Prog. Solid State Chem.* **20**, 1–45.
- Park, S.-M., Kim, S.-J. & Kanatzidis, M. G. (2003). *J. Solid State Chem.* **175**, 310–315.
- Pfuner, F., Degiorgi, L., Ott, H.-R., Bianchi, A. & Fisk, Z. (2008). *Phys. Rev. B*, **77**, 024417.
- Shannon, R. D. (1976). *Acta Cryst.* **A32**, 751–767.
- Sheldrick, G. M. (2003). *SADABS*. University of Göttingen, Germany.
- Sheldrick, G. M. (2008). *Acta Cryst.* **A64**, 112–122.
- Somer, M., Carrillo-Cabrera, W., Peters, K. & von Schnering, H. G. (1998). *Z. Kristallogr.* **213**, 4.
- Xia, S. Q. & Bobev, S. (2007). *J. Am. Chem. Soc.* **129**, 10011–10018.
- Xia, S. Q. & Bobev, S. (2008). *Inorg. Chem.* **47**, 1919–1921.